Trivalent Ion Hydrolysis Reactions II: Analysis of Electron Density Distributions in Metal−Oxygen Bonds

Kevin M. Rosso,*,† James R. Rustad,† and G. V. Gibbs‡

W.R. Wiley Environmental Molecular Sciences Laboratory, Pacific Northwest National Laboratory, Richland, Washington 99352, and Departments of Geological Sciences, Materials Sciences, and Mathematics, Virginia Polytechnic Institute and State University, Blacksburg, Virginia 24061

Received: January 11, 2002; In Final Form: April 23, 2002

Density functional theory calculations are applied to a series of trivalent hexaquo metal complexes to determine whether systematic properties exist in the electron density distribution of the metal−oxygen (M−O) bonds in relation to the proton binding energy. Bader metal ion charges, radii, and M−O bond critical point properties are computed and correlations are sought that transcend conventionally ascribed factors affecting hydrolysis behavior, such as position in the periodic table and d-orbital filling. Charge-to-radius relationships are found to be unimproved by these methods. At the M−O bond critical points, while no correlation could be established with the electron density, distinct trends in the proton binding energy are unveiled by the Laplacian, owing principally to systematics in the curvature $|\lambda_3|$ along the M−O bond path. The ellipticity of the bonds can reflect a π interaction between the metal cation and water ligands for metal cations in which the t_{2g} d-orbital set is asymmetrically occupied, which is found to be coupled with a symmetry-breaking rotation of the ligands. Although global correlations were not found, the trends establish quantities that can uniquely connect hydrolysis behavior across traditional classification factors.

1. Introduction

Hydrolysis is a fundamentally important process that can significantly transform the chemical behavior of metal ions in aqueous solution. For example, coordinating hydroxide ions typically enhance the labilization of coordinating water molecules in hydrolyzed complexes[1] and stabilize oxidized products in electron-transfer reactions involving hydrolyzed reductants.[2−4] The need to improve our ability to predict the stabilities of various hydrolysis products has motivated theoretical efforts to identify factors that can help unify predictive models.

Achieving this objective has been a particularly difficult task for trivalent metal ions. The hydrolyzing ability of a metal ion is roughly proportional to the charge to ionic radius ratio,[5] but no general approach such as this has completely succeeded in correlating the hydrolysis constants of all of the trivalent ions.[6] For transition-series trivalent ions, electronic structure effects arising from the filling of d orbitals for the transition metal ions play a large role in degrading the success of simpler correlations, but even within a transition series, d-orbital filling alone does not appear to be a satisfactory unifying factor.[7] Recent studies have relied on electronic structure calculations such as density functional theory (DFT) methods to inherently capture such effects.[8−13] Cluster calculations of absolute pK_{11}[14] show that calculated pK_{11}'s can converge to observed values by increasing the number of explicitly treated hydration shells in the complex, but including both the first and second hydration shells explicitly leads to only moderately satisfactory values.[8] Indeed, others have demonstrated similar problems owing to difficulties in the explicit calculation of solvent effects.[9−12] A different strategy is to develop linear free energy relationships between the relative acidities of a series of relatively small metal−water clusters in the gas phase with the values of the hydrolysis constants.[9,13] The success of this strategy relies on the cancellation of solvent effects.

What remains hidden in these strategies is a portrayal of the underlying effects of the electronic structure that lead to their hydrolysis behavior. Clearly a more broadly reaching correlation will require the identification of factors that can transcend d-orbital occupation. Towards that end, we not only extend previous calculations[13] but scrutinize the calculated electronic structure of M−O bonds in the trivalent ion clusters for systematic properties influencing the acidity of the ions. To do this in a way that is potentially least obstructive to the possibility of finding more comprehensive models, we take the perspective that electronic effects that could be analyzed using molecular orbital models will also manifest themselves as changes in the electron density distribution. We performed a bond critical point analysis of the electron density distributions for Al^{3+}, Sc^{3+}, Ti^{3+}, V^{3+}, Cr^{3+}, Mn^{3+}, Fe^{3+}, Ga^{3+}, Y^{3+}, Ru^{3+}, Rh^{3+}, and In^{3+} hexaquo ions and utilize the framework forged by Bader and co-workers[15] in an attempt to gain additional insight into the origins of trivalent ion hydrolysis behavior.

Bader[15] showed that many properties and an understanding of the reactivities of a large variety of molecules can be obtained by evaluating the gradient field, $\nabla\rho(\mathbf{r})$, and the Laplacian, $\nabla^2\rho(\mathbf{r})$, of the electron density distributions. For example, it was found that $\nabla\rho(\mathbf{r})$ provides a basis for defining chemical bonds, atoms in molecules, and the net charges of the atoms. A bond path is defined as a line of atomic interaction along a ridge of electron density that connects the peaks of electron density at the positions of two bonded atoms. The point along the crest of the ridge where $\rho(\mathbf{r})$ is a minimum defines a saddle critical point where $\nabla\rho(\mathbf{r}) = 0$. Unique positions such as this are termed

* To whom correspondence should be addressed. E-mail: kevin.rosso@pnl.gov.
† Pacific Northwest National Laboratory.
‡ Virginia Polytechnic Institute and State University.

10.1021/jp020075k CCC: $22.00
Published on Web 08/03/2002

critical points, which are denoted here by the position $\mathbf{r}_c$. Critical point types are classified by the rank and signature of the Hessian matrix of ρ, which has eigenvalues denoted λ_1, λ_2, and λ_3. A bond critical point (bcp) described above is denoted a (3, −1) critical point. The quantities $|\lambda_1|$ and $|\lambda_2|$ define the curvatures of $\rho(\mathbf{r}_c)$ along two mutually perpendicular eigenvectors each oriented perpendicular to the bond path. The third, $|\lambda_3|$, defines the curvature along an eigenvector directed along the bond path. The sum of λ_1, λ_2, and λ_3 equals $\nabla^2\rho(\mathbf{r})$, which is an indication of where $\rho(\mathbf{r})$ is locally greater than or less than that, on average, in the immediate vicinity of $\mathbf{r}$.[15] The distance between each atom in a bonded pair and $\mathbf{r}_c$ defines the bonded radii of the atoms. Because the position of $\mathbf{r}_c$ is usually situated closer to the more electropositive atom, it also provides a measure of the polarity of the bond and can closely parallel trends in bond covalency.

The gradient vector field of the electron density distribution of a molecule also provides a basis for defining atoms and their net charges.[15,16] Starting in any direction from the nucleus of an atom, one can follow a gradient path in the direction of $\nabla\rho(\mathbf{r})$ that either continues indefinitely or terminates at a critical point. The space traversed by all such paths originating at a particular atom nucleus is defined to be the basin of that atom. The average electron population of the atom is found by integrating $\rho(\mathbf{r})$ over the basin of the atom, with the net charge resulting from the sum of its nuclear charge and its electron population.

By evaluation of the properties of the electron density distributions at the bcp between bonded atoms, valuable information can be obtained including bond type and order, partial π-bond character, electron delocalization, bent bond character, strain energy, and bonds that are susceptible to cleavage. For example, the value of $\lambda_1/\lambda_2 - 1$ is a useful description of the ellipticity (ϵ) of a bond, with high ϵ ascribed to either the formation of π-bond character or, where ϵ is unusually large, a highly strained bond that is susceptible to rupture.[15,17] A sharp positive curvature of the electron density (a large λ_3 value) along a bond path at $\mathbf{r}_c$ is believed to reflect a "stiffness" of the bond and a resistance to change. On the other hand, a bond with a large accumulation of electron density at $\mathbf{r}_c$ and a smaller curvature of the electron density is believed to be less resistant to change and more easily perturbed.[15] A great triumph of the theory is its ability to treat both individual atoms and bonded atoms in molecules and in solids on an equal footing. Here, we apply these concepts to better understand the energetics of trivalent metal ion hydrolysis.

2. Theoretical Methods

DFT calculations were performed on $M(H_2O)_6^{3+}$ and $M(OH)(H_2O)_5^{2+}$ complexes for the trivalent metals listed above using Gaussian 98.[18] The ions are, for the most part, experimentally observed to be hexacoordinated in aqueous solution.[6] Sc^{3+} and Y^{3+} have coordination numbers higher than six,[19−22] but they are treated as $M(H_2O)_6^{3+}$ ions to eliminate the systematic size dependence for removal of a proton from a gas-phase cluster and to maintain equality in the cancellation of solvent effects. The theory level, basis sets, optimization strategy, and definition of the proton binding energy (ΔE_{H^+}) are similar to previous calculations.[13] We use

$$\Delta E_{H^+} = [E(M(OH)(H_2O)_5^{2+}) + ZPE(M(OH)(H_2O)_5^{2+})] - [E(M(H_2O)_6^{3+}) + ZPE(M(H_2O)_6^{3+})]$$

where E refers to the total electronic energy and ZPE refers to the zero-point energy correction. We calculate the average binding energy of a water molecule to each metal atom (ΔE_{H_2O}) using

$$\Delta E_{H_2O} = \{[E(M^{3+}) + 6E(H_2O)] - E(M(H_2O)_6^{3+})\}/6$$

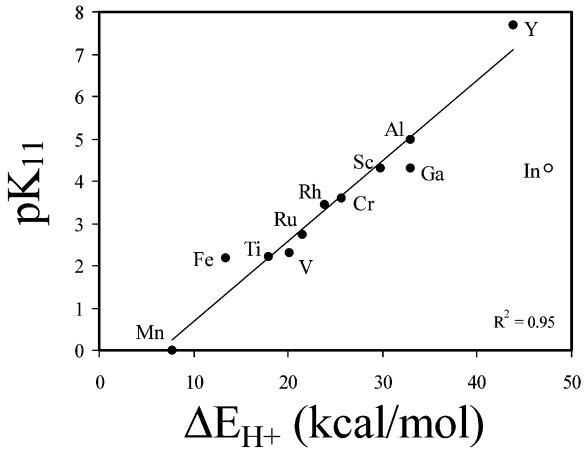

Figure 1. Plot of observed pK_{11} values (sources tabulated in ref 13) against proton binding energies calculated in this study. Note that pK_{11} for Mn^{3+} was incorrectly cited in ref 13. Here we use $pK_{11} = 0.0$ for Mn^{3+}.[37]

Geometries were optimized without symmetry constraints using analytic gradient methods at the local level with the exchange potential fit of Slater[23−25] and the correlation potential fit of Vosko, Wilk, and Nusair.[26] Final energies for the optimal LDFT structures were calculated at the gradient-corrected level with Becke's three-parameter hybrid DFT method (UB3LYP),[27] which includes both Hartree−Fock and DFT exchange, and the Lee−Yang−Parr correlation functional.[28] This represents a slight change with respect to previous methods,[13] motivated by the desire to check for systematic differences in the computed energies that may originate from the choice of DFT method. The optimizations were done with DZVP2 basis sets where possible (Al, Fe, Ti, V, Sc, Cr, Mn, O, H) and with DZVP basis sets (Ga, Y, Ru, Rh, In) otherwise.[29−32] These are nonrelativistic, all-electron, polarized DFT orbital basis sets based on the local spin density approximation. All calculations were carried out for the high-spin case for complexes with occupied d orbitals, except for Ru^{3+} and Rh^{3+}, which are experimentally observed to be low-spin under ambient solution conditions.[6] Topological analyses of the electron density distribution and net charge calculations based on the final wave functions were performed using the XTREM and PROAIMV codes, respectively, in the AIMPAC series of programs,[33] generously supplied by Richard Bader and his research associates in the Chemistry Department at McMaster University.

3. Results and Discussion

Of primary interest in this study was to see whether the properties of the electron density distributions at any of the six M−O bcp's in each $M(OH_2)_6^{3+}$ ion can be correlated with the calculated energy to remove a proton. Computed energies and average bcp properties are given in Table 1. We first demonstrate that the addition of Ru^{3+} and Rh^{3+} ions lends further credence to the correlation between observed pK_{11} and the calculated proton binding energy ΔE_{H^+} in Figure 1. When it is noted that that their d-orbital electronic configurations are both observed and were therefore modeled as low-spin, as opposed to the remaining ions, which are high spin, additional support for the observed low-spin assignment is provided by the

TABLE 1: Calculated Water and Proton Binding Energies, d-Orbital Configurations, Average Bond Lengths, and Average Properties of the Electron Density Distributions at the Bond Critical Points in the Six M−O Bonds for Each Trivalent Hexaquo Ion[a]

3+ ion	ΔE_{H_2O} (kcal/mol)	ΔE_{H^+} (kcal/mol)	d-shell config.	avg M−O (Å)	avg r(M) (Å)	metal net chrg	avg $\rho(\mathbf{r}_c)$ (e^-/Å^3)	avg λ_1 (e^-/Å^5)	avg λ_2 (e^-/Å^5)	avg λ_3 (e^-/Å^5)
Al	117.0	32.9	N/A	1.909	1.112	2.62	0.397	−2.312	−2.142	13.492
Sc	92.6	29.8	$t_{2g}^0e_g^0$	2.118	1.051	2.25	0.426	−2.468	−2.176	12.226
Ti	105.1	18.0	$t_{2g}^1e_g^0$	2.049	1.028	2.15	0.477	−2.658	−2.108	14.454
V	113.4	20.1	$t_{2g}^2e_g^0$	2.001	1.015	2.04	0.515	−2.703	−1.915	16.037
Cr	126.4	25.7	$t_{2g}^3e_g^0$	1.963	1.007	1.93	0.552	−2.329	−2.061	17.231
Mn	122.9	7.7	$t_{2g}^3e_g^1$	1.990	1.010	1.88	0.563	−2.785	−2.491	15.907
Fe	120.6	13.3	$t_{2g}^3e_g^2$	2.011	1.014	1.83	0.545	−2.820	−2.505	13.463
Ga	118.6	32.9	$t_{2g}^6e_g^4$	1.970	1.005	2.03	0.570	−3.047	−2.796	14.059
Y	76.4	43.8	$t_{2g}^0e_g^0$	2.297	1.093	2.40	0.358	−1.757	−1.544	8.990
Ru	121.5	21.5	$t_{2g}^5e_g^0$	2.044	0.998	1.68	0.584	−1.938	−1.267	15.830
Rh	132.5	23.8	$t_{2g}^6e_g^0$	2.024	0.991	1.56	0.612	−1.713	−1.598	16.388
In	96.3	47.5	$t_{2g}^6e_g^4$	2.168	1.053	2.19	0.447	−1.998	−1.823	11.191

[a] Deviations from the average values are small except for Mn^{3+} for which large Jahn−Teller distortions lead to distinctly different properties for different pairs of Mn−O bonds. Ru^{3+} and Rh^{3+} are treated as low-spin complexes, whereas other partially occupied d-shell complexes are treated as high-spin ones, consistent with experimental observation.

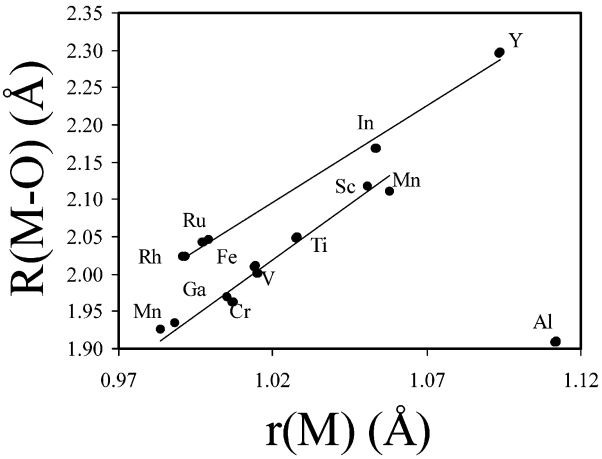

Figure 2. Calculated M−O bond lengths compared against metal radii calculated as the distances from the metal nuclei to metal−oxygen bcp's.

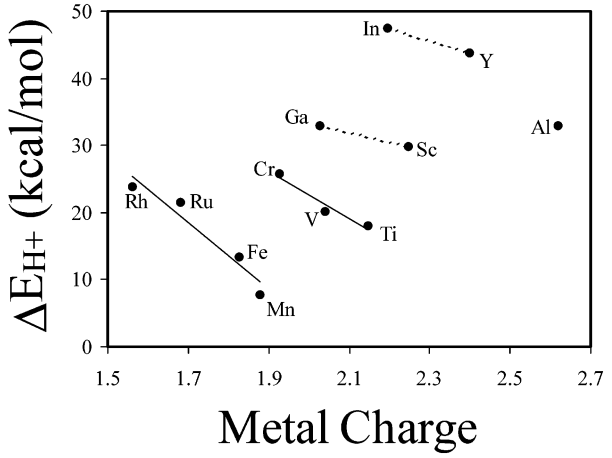

Figure 3. Proton binding energies vs the net charge on metal atoms calculated using Bader's methods.

correlation in Figure 1. At the same time, it extends a previous conclusion[13] that DFT methods are able to describe effects that the electronic and spin structure of the complex may have on the basicities of the M^{3+}−OH interactions. However, poor agreement with the correlation is found for In^{3+}, a complex for which measurement of hydrolysis constants are apparently not overly hindered by the presence of polynuclear species.[7] Given its predicted similarities with pK_{11} for Sc^{3+}, the calculated ΔE_{H^+} for In^{3+} seems to be too high. The cause for the overestimate of the proton binding energy for In^{3+} is unclear, but it is conceivable that it could at least be in part due to the neglect of relativistic effects[34,35] for this, the largest core metal of all of the considered metal ions. In^{3+} is treated as an outlier in Figure 1, but its bcp properties are included in subsequent discussions because systematic behavior of some of these properties with ΔE_{H^+} is apparently retained.

Some of the more "straightforward" computed properties such as the net charge on the metal atom (Z), the calculated radii of the metal atoms (r(M)), and their ratio (Z/r(M)) were found not to correlate uniformly with ΔE_{H^+}. This is consistent with the idea that electronic effects probably play a large role in degrading such simple correlations that could exist for the trivalent ions. However, these properties were found to be internally related to one another in a relatively intuitive manner. For example, the M−O bond length R(M−O) was found to correlate with r(M) (Figure 2). In this trend, a linear increase in R(M−O) with an increasing size of the metal atom can clearly be seen, with a dependence on the row number in the periodic table. Noting that all six bond lengths in each complex are plotted in Figure 2, a large disparity between bond pairs in Mn^{3+} can be seen. This is due to large Jahn−Teller distortions from the asymmetric occupation of e_g* orbitals, which interact strongly with the octahedrally arranged ligands. This breaks Mn−O bonds into pairs of differing length. All other complexes showed either no such distortions or ones much smaller in magnitude arising from weaker Jahn−Teller effects due to asymmetric occupation of t_{2g} orbitals, which point along directions between the ligands.

Although a uniform correlation was not found between ΔE_{H^+} and Bader charges on the metal atoms, groupings of trends were found (Figure 3). The groups are defined by both a dependence on position in the periodic table and the filling structure of d orbitals. The first and second row transition series end members, Ga^{3+}/Sc^{3+} and In^{3+}/Y^{3+}, respectively, are arranged similarly relative to one another in Figure 3, with the offset between these two groups presumably due to the difference in core size. Similarly sloped lines can be superimposed on two other groups of $Cr^{3+}/V^{3+}/Ti^{3+}$ and $Rh^{3+}/Ru^{3+}/Fe^{3+}/Mn^{3+}$, with the latter notably incorporating metals from both the first and second transition series. The underlying difference between these last two groups is in the occupation of e_g* orbitals, with the former having no e_g* electrons and the latter having at least one e_g* electron (see Table 1). Within each group, ΔE_{H^+} increases with increasing numbers of d electrons. Al^{3+} does not conform with

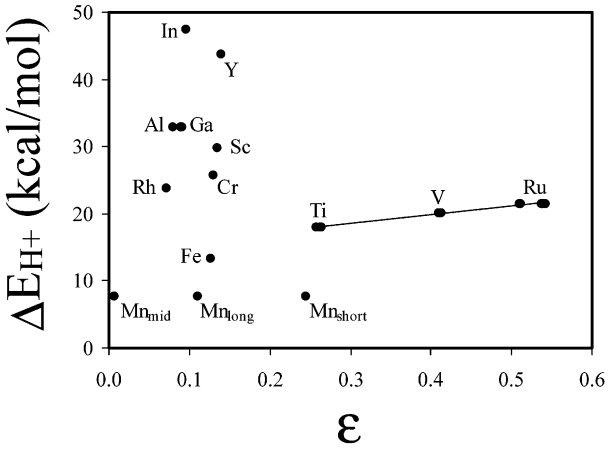

Figure 4. Proton binding energies vs the ellipticity (ϵ) of metal−oxygen bonds at bcp's calculated using the ratio $\lambda_1/\lambda_2 - 1$.

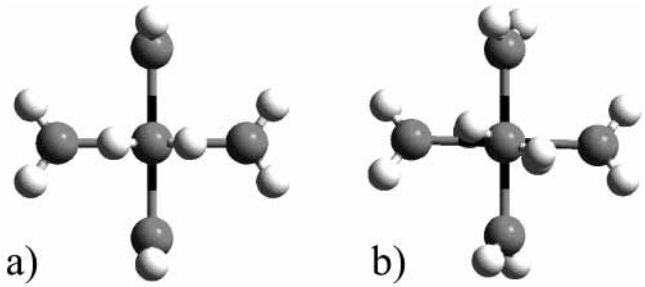

Figure 5. Ball-and-stick models showing the preferred ligand orientations for (a) Al^{3+}, Sc^{3+}, Cr^{3+}, Mn^{3+}, Fe^{3+}, Ga^{3+}, Y^{3+}, Ru^{3+}, Rh^{3+}, and In^{3+} and (b) Ti^{3+}, V^{3+}, and Ru^{3+}. Metals in the former group possess either no t_{2g} d orbitals or symmetrically filled ones, resulting in T_h symmetry, and the metals in the latter group have asymmetrically filled t_{2g} d orbitals, resulting in water ligand rotation and D_3 symmetry.

any of these groupings because it lacks a d shell. Collectively, these observations hint at some of the effects that d-orbital configuration can have on proton binding energies. Extending this conclusion much further is hampered by the limited number of ions for which a $M(OH_2)_6^{3+}$ calculation makes sense.

Additional insight into the effects of d-orbital configuration is demonstrated by plotting ΔE_{H^+} against the ellipticity ϵ for the M−O bonds at $\mathbf{r}_c$ (Figure 4). While no trends relating ΔE_{H^+} to the curvatures λ_1 or λ_2 are apparent, a trend between ΔE_{H^+} and ϵ can be seen and rationalized for a small fraction of the ions. Here, we find for the most part no perceivable correlation except for the three ions Ti^{3+}, V^{3+}, and Ru^{3+}. In seeking explanations based on their electronic structure, we find that these three ions share the unique quality within the entire metal series considered that their t_{2g} set of d orbitals are asymmetrically filled ($Ti^{3+} = 3d^1$, $V^{3+} = 3d^2$, $Ru^{3+} = 4d^5$ low spin). Coupled with this is the observation that the optimized structures for these three ions in particular show that their water ligands prefer to undergo a rotation on the octahedral axes (Figure 5). The average dihedral angles describing this out-of-plane rotation for the final structures are 22.0° (Ti^{3+}), 12.3° (V^{3+}), and 22.3° (Ru^{3+}). Because symmetry constraints were not imposed during optimizations, this motion breaks the final symmetry from T_h to D_3, whereas all other ions converged to T_h. We conclude that the systematics in ϵ, the feature of asymmetrically filled t_{2g} orbitals, and the out-of-plane rotation of the water ligand for Ti^{3+}, V^{3+}, and Ru^{3+} are related properties. Previous studies of have established relationships between ϵ and either partial π-bonding character or strain in a bond.[15,17] Because resistance

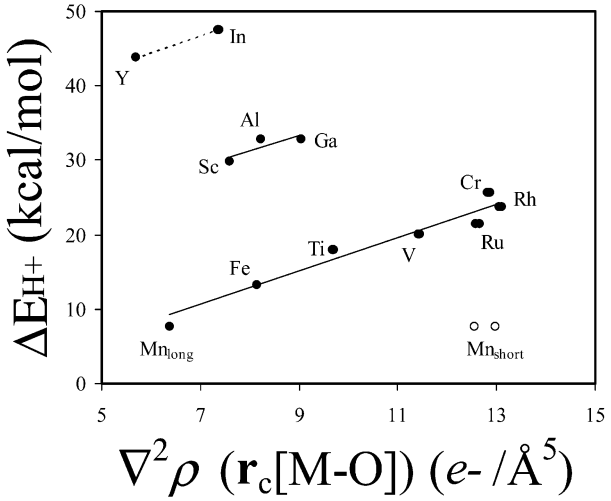

Figure 6. Proton binding energies vs the Laplacian of the electron density evaluated at the bcp's of the M−O bonds.

to rotational motion of the water ligands is expected to be relatively weak compared to bond length modification and because this rotation would increase overlap between the occupied π orbitals on H_2O with the t_{2g} orbitals, we assume that the behavior that we find for Ti^{3+}, V^{3+}, and Ru^{3+} is principally an indication of π-like interaction between the metal atom and water ligands. Although the influence of M−O bond ellipticity on ΔE_{H^+} is apparent, and possibly plays a role in the hydrolysis of certain divalent ions as well, the degree of dependence of ΔE_{H^+} on ϵ is nevertheless is small as can be seen from the shallow slope of the line with respect to the scatter along the *y*-axis in Figure 4. We therefore conclude that this effect is relatively minor.

No trend could be discerned between ΔE_{H^+} and $\rho(\mathbf{r}_c[M-O])$, but interestingly, ΔE_{H^+} showed clear relationships with the Laplacian $\nabla^2\rho(\mathbf{r}_c[M-O])$ (Figure 6). Groupings of linear trends could be found differentiated from each other by d-orbital occupation and position in the periodic table. The principal trend observed incorporates all partially filled d-shell ions, Ti^{3+}, V^{3+}, Cr^{3+}, Mn^{3+}, Fe^{3+}, Ru^{3+}, and Rh^{3+}. Secondary trends with lines of similar slope for a group consisting of Al^{3+}, Sc^{3+}, and Ga^{3+} and also of Y^{3+} and In^{3+} were found, with the latter suffering from a lack of possible additional similar ions. In general within each group, ΔE_{H^+} tends to increase with an increasing number of d electrons, with the exception of Mn^{3+} and Fe^{3+}, which are different in that they both have partially occupied e_g* orbitals. Because these orbitals interact strongly with the ligands in the octahedral case, it seems possible that this occupation can uniquely affect the M−O interaction and therefore hydrolysis behavior.

The trends between ΔE_{H^+} and $\nabla^2\rho(\mathbf{r}_c[M-O])$ possess several intriguing qualities. First is the ability of $\nabla^2\rho(\mathbf{r}_c[M-O])$ to correlate ions across different rows in the periodic table, such as the grouping of Al^{3+} with first transition series ions Sc^{3+} and Ga^{3+} and also the grouping of the second transition series ions Ru^{3+} and Rh^{3+} with first transition series ions Mn^{3+}, Fe^{3+}, Ti^{3+}, V^{3+}, and Cr^{3+}. Both groupings combine metal ions across well-established metal ion groupings based on various Z/r relationships.[7,36] For example, Al^{3+} lies on a different Z/r trend than Sc^{3+} and Ga^{3+},[7] and the second transition series metal ions are thought to be necessarily treated separately from the first transition series ions because of differences in electronegativity.[36] The trends observed in Figure 6 seem to be unique in that they segregate the metal ions with partially filled d orbitals and exclude other d-orbital bearing ions.

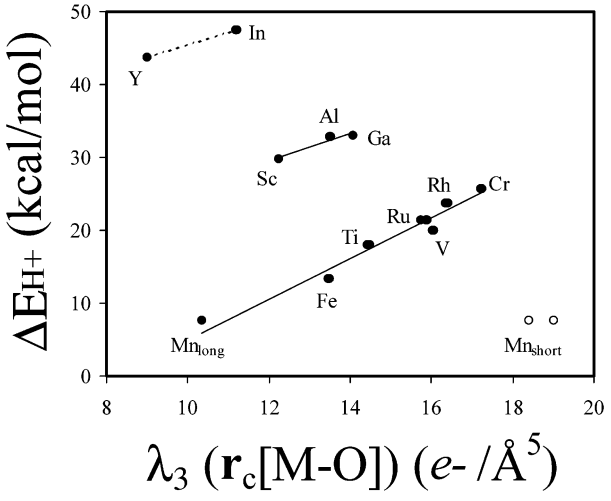

Figure 7. Calculated proton binding energies vs λ_3, the curvature along the bond path, evaluated at the bcp's of the M−O bonds.

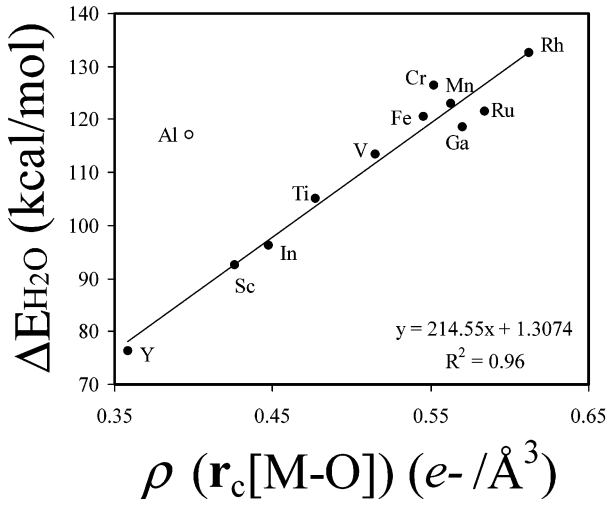

Figure 8. Average water binding energies vs the average electron density evaluated at the bcp's of the M−O bonds.

The second intriguing quality is specific to Mn^{3+}. Only $\nabla^2\rho(\mathbf{r}_c[M-O])$ corresponding to the longest bond pair in Mn^{3+} lies on the ΔE_{H^+} trend, whereas the shorter Mn^{3+} bond pairs are distinctly off-trend (Figure 6). Under the assumption that Mn^{3+} does indeed belong in the grouping of ions similar to it, this might be taken to suggest that Mn^{3+} hydrolysis behavior arises from water ligands located *furthest* away from the Mn^{3+} center. This would be in conflict with the well-established observation that the closer water is held to the metal ion, the easier it becomes to remove one of its protons.[7] We tested this hypothesis by running two additional total energy calculations on the frozen optimized $Mn(OH_2)_6^{3+}$ structure minus a proton from two different water ligands. In one case, a proton was taken from a water ligand on one of the two long Mn−O bonds, and in the other case, it was taken from a water ligand on one of the short Mn−O bonds. The latter choice was lower in energy by 18.4 kcal/mol, consistent with a greater ease of proton removal from water ligands closer to the metal center. Therefore, we conclude that the energetics of Mn^{3+} hydrolysis is uniquely separate from the ΔE_{H^+} vs λ_3 trend observed for the other partially occupied d-orbital metal ions. This is consistent with similar anomalous behavior deduced as a result of efforts to fit an empirical relationship based on an extension of Z/r relationships over a wide range of experimental hydrolysis constants.[36]

Although the value of $\nabla^2\rho$ has been shown to equate to local concentrations and depletions in the electron density distribution, it is not immediately clear how to or even whether it would be valuable to connect these concepts to d-orbital occupation, a characteristic that seems to weigh heavily on the hydrolysis energetics of these ions. These types of detailed connections must await further development of the Bader's theory, for which there currently seems to be very little application to transition metal complexes. Nevertheless, for the ions in this study, it can be shown that λ_3 is the most important eigenvector component of $\nabla^2\rho(\mathbf{r}_c[M-O])$, and that it captures at least in part aspects of the electronic properties affecting hydrolysis (Figure 7). As already mentioned, ΔE_{H^+} shows no correlation with λ_1 or λ_2, but ΔE_{H^+} vs λ_3 can be seen to be very similar to ΔE_{H^+} vs $\nabla^2\rho(\mathbf{r}_c[M-O])$. The curvature in the electron density described by λ_3 is that oriented along the bond path. λ_3 has been useful to characterize charge transfer between bonded atoms, in analogy with ionic vs covalent considerations, and bond stiffness.[15] A large positive value at $\mathbf{r}_c$ is indicative of sharply peaked positive curvature in the electron density along a bond. For a particular bonded pair, an increasing λ_3 has been tied to the preferential accumulation of charge in the atomic basins of the bonded pair, in analogy with a decrease in the covalent character of a bond.[15] Also, increasing λ_3 can reflect an increase in the resistance of a particular bond to change.

For the M−O bonds in this study, it is difficult to precisely know what property of the bonds is manifested in the λ_3 trend. It may be asked whether λ_3 is capturing a systematic change in M−O bond strength. An increasing M−O bond strength might be expected to decrease O−H bond strengths and cause ΔE_{H^+} to decrease. We have addressed this question by computing the average binding energy for a water ligand to each trivalent metal atom in the hexaquo complexes (ΔE_{H_2O}) and comparing these values with bcp properties of the M−O bonds (Table 1). We find that, for all of the complexes except Al, ΔE_{H_2O} is linearly correlated with $\rho(\mathbf{r}_c[M-O])$ with a y-intercept of nearly zero (Figure 8). From this, we conclude that the M−O bond strength is directly related to the electron density at the bcp. However, no correlation was found to exist between ΔE_{H_2O} and ΔE_{H^+}. Therefore, ΔE_{H^+} is not systematically tied to M−O bond strength. The quantity λ_3 appears to reflect some other property of M−O bonds that influences ΔE_{H^+}, a property that remains unidentified. Drawing a detailed conclusion along these lines is somewhat disadvantaged by the fact that we are making comparisons across different M−O bonds as they occur in a similar structural configuration (e.g., $Fe-O_{oct}$, $Mn-O_{oct}$, $Cr-O_{oct}$, etc.), as opposed to comparing the properties of the same M−O bond pair in a variety of structural configurations ($Fe-O_{tet}$, $Fe-O_{oct}$, etc.). Nevertheless, it is clear that systematics are present in λ_3 that possibly capture the influence of electronic effects on the energetics of trivalent metal ion hydrolysis.

4. Summary and Conclusions

Although properties of the electron density distribution at M−O bond critical points do not globally unify the hydrolysis energetics of the common trivalent hexaquo ions, certain quantities did show a capacity to transcend conventional classification factors such as position in the periodic table and Z/r relationships. The curvature of the electron density along the bond path λ_3, a quantity that was previously related to bond stiffness, appears to capture electronic effects on hydrolysis arising from partially filled d orbitals. An increase in λ_3 at the bond critical point along M−O bonds is tied to an increase in the energy to remove a proton from the metal−water complex. Trends of lesser influence on ΔE_{H^+} were found for metal ions

with an asymmetric occupation of t_{2g} d orbitals, whereby partial π-bonding interactions are established between t_{2g} orbitals and water ligands, accompanied by an out-of-plane rotation of water ligands on the octahedral axes. This behavior is captured in the Bader definition of bond ellipticity for the M−O bonds in these complexes. In agreement with previous observations, the relationship between d-orbital filling and hydrolysis for the Mn^{3+} hexaquo ion is found to be anomalous, likely owing to strong Jahn−Teller distortions in this complex.

Acknowledgment. Pacific Northwest National Laboratory is operated for the U.S. Department of Energy by Battelle Memorial Institute under Contract DE-AC06-76RL0 1830. We are grateful to the National Energy Research Supercomputing Center for a generous grant of computer time. Special thanks to J. J. Morgan for useful discussions regarding the hydrolysis constant for Mn^{3+}.

References and Notes

(1) Nordin, J. P.; Sullivan, D. J.; Phillips, B. L.; Casey, W. H. *Inorg. Chem.* **1998**, *37*, 4760.

(2) Sedlak, D. L.; Chan, P. G. *Geochim. Cosmochim. Acta* **1997**, *61*, 2185.

(3) Fendorf, S. E.; Li, G. *Environ. Sci. Technol.* **1996**, *30*, 1614.

(4) Eary, L. E.; Rai, D. *Am. J. Sci.* **1989**, *289*, 180.

(5) Huheey, J. E. *Inorganic Chemistry*, 3rd ed.; Harper and Row: New York, 1983.

(6) Richens, D. T. *The Chemistry of Aquo Ions*; John Wiley and Sons: New York, 1997.

(7) Baes, C. F.; Mesmer, R. E. *Hydrolysis of Cations*; Robert E. Krieger Publishing Company: Malabar, FL, 1976.

(8) Li, J.; Fisher, C. L.; Chen, J. L.; Bashford, D.; Noodleman, L. *Inorg. Chem.* **1996**, *35*, 4694.

(9) Tossell, J. A.; Sahai, N. *Geochim. Cosmochim. Acta* **2000**, *64*, 4097.

(10) Rustad, J. R.; Hay, B. P.; Halley, J. W. *J. Chem. Phys.* **1995**, *102*, 427.

(11) Rustad, J. R.; Hay, B. P. *Geochim. Cosmochim. Acta* **1995**, *59*, 1251.

(12) Martin, R. L.; Hay, P. J.; Pratt, L. R. *J. Phys. Chem. A* **1998**, *102*, 3565.

(13) Rustad, J. R.; Dixon, D. A.; Rosso, K. M.; Felmy, A. R. *J. Am. Chem. Soc.* **1999**, *121*, 3234.

(14) We use the notation pK_{xy} to mean $-\log K_{xy}$, where $K_{11} = [M^{z+}{}_x(OH)_y{}^{(xz-y)+}][H^+]^y/[M^{z+}]^x\gamma_{MOH^{(xz-y)+}}\gamma_{H^+}{}^y/\gamma_{M^{z+}}{}^x a H_2O^y$ as defined on page 10 of ref 7. pK_{11} refers to the first hydrolysis constant of the mononuclear species.

(15) Bader, R. F. W. *Atoms in Molecules: A Quantum Theory*; Oxford University Press: Oxford, U.K., 1990.

(16) Bader, R. F. W. *Chem. Rev.* **1991**, *91*, 893.

(17) Kraka, E.; Cremer, D. In *The Concept of the Chemical Bond*; Maskíc, Z. B., Ed.; Springer-Verlag: Berlin, Germany, 1990.

(18) Frisch, M. J.; Trucks, G. W.; Schlegel, H. B.; Scuseria, G. E.; Robb, M. A.; Cheeseman, J. R.; Zakrzewski, V. G.; Montgomery, J. A., Jr.; Stratmann, R. E.; Burant, J. C.; Dapprich, S.; Millam, J. M.; Daniels, A. D.; Kudin, K. N.; Strain, M. C.; Farkas, O.; Tomasi, J.; Barone, V.; Cossi, M.; Cammi, R.; Mennucci, B.; Pomelli, C.; Adamo, C.; Clifford, S.; Ochterski, J.; Petersson, G. A.; Ayala, P. Y.; Cui, Q.; Morokuma, K.; Malick, D. K.; Rabuck, A. D.; Raghavachari, K.; Foresman, J. B.; Cioslowski, J.; Ortiz, J. V.; Stefanov, B. B.; Liu, G.; Liashenko, A.; Piskorz, P.; Komaromi, I.; Gomperts, R.; Martin, R. L.; Fox, D. J.; Keith, T.; Al-Laham, M. A.; Peng, C. Y.; Nanayakkara, A.; Gonzalez, C.; Challacombe, M.; Gill, P. M. W.; Johnson, B. G.; Chen, W.; Wong, M. W.; Andres, J. L.; Head-Gordon, M.; Replogle, E. S.; Pople, J. A. *Gaussian 98*, revision A.4; Gaussian, Inc.: Pittsburgh, PA, 1998.

(19) Ohtaki, H.; Radnai, T. *Chem. Rev.* **1993**, *93*, 1157.

(20) Kanno, H.; Yamaguchi, T.; Ohtaki, H. *J. Phys. Chem.* **1989**, *93*, 1695.

(21) Yamaguchi, T.; Niihara, M.; Takamuku, T.; Wakita, H.; Kanno, H. *Chem. Phys. Lett.* **1997**, *274*, 485.

(22) Cabaco, M.; Marques, M. A.; Marques, M. I. de B.; Bushnell-Wye, G.; Costa, M. M.; de Almeida, M. J.; Andrade, L. C. *J. Phys.: Condens. Matter* **1995**, *7*, 7409.

(23) Hohenberg, P.; Kohn, W. *Phys. Rev.* **1964**, *136*, B864.

(24) Kohn, W.; Sham, L. J. *Phys. Rev.* **1965**, *140*, A1133.

(25) Slater, J. C. *Quantum Theory of Molecules and Solids v. 4: The Self-Consistent Field for Molecules and Solids*; McGraw-Hill: New York, 1974.

(26) Vosko, S. H.; Wilk, L.; Nusair, M. *Can. J. Phys.* **1980**, *58*, 1200.

(27) Becke, A. D. *J. Chem. Phys.* **1993**, *98*, 5648.

(28) Lee, C.; Yang, W.; Parr, R. G. *Phys. Rev. B* **1988**, *37*, 785.

(29) Andzelm, J.; Wimmer, E.; Salahub, D. R. In *The Challenge of d and f Electrons: Theory and Computation*; Salahub, D. R., Zerner, M. C., Eds.; ACS Symposium Series 394; American Chemical Society: Washington, DC, 1989; p 228.

(30) Andzelm, J. In *Density Functional Theory in Chemistry*; Labanowski, J., Andzelm, J., Eds.; Springer-Verlag: New York, 1991; p 155.

(31) Andzelm, J.; Wimmer, E. *J. Chem. Phys.* **1992**, *96*, 1280.

(32) Godbout, N.; Salahub, D. R.; Andzelm, J.; Wimmer, E. *Can. J. Chem.* **1992**, *70*, 560.

(33) Biegler-König, F. W.; Bader, R. F. W.; Tang, T. H. *J. Comput. Chem.* **1982**, *13*, 317.

(34) Bauschlicher, C. W. *Chem. Phys. Lett.* **1999**, *305*, 446.

(35) Schwerdtfeger, P.; Fischer, T.; Dolg, M.; Igelmann, G.; Nicklass, A.; Stoll, H.; Haaland, A. *J. Chem. Phys.* **1995**, *102*, 2050.

(36) Brown, P. L.; Sylva, R. N.; Ellis, J. *J. Chem. Soc., Dalton Trans.* **1985**, 723.

(37) Macartney, D. H.; Sutin, N. *Inorg. Chem.* **1985**, *24*, 3403.